AVIATION 2014, AIAA Aviation and Aeronautics Forum and Exposition, 16–20 June 2014, Hyatt Regency Atlanta, Atlanta, Georgea

# Generation of Normalized Difference Vegetation Index Map for Precision Agriculture Using Small-Type Unmanned Aerial Vehicle

Kazuhisa Chiba[*], Takuya Kamei[†], Tomonori Ito[†], Shin-ya Sugai[†], Satoshi Ohta[‡], and Shin Satori[§]
*Hokkaido University of Science, Sapporo 006-8585, Japan*

**Precision agriculture has been implemented in order to environmentally friendly and efficiently product and manage crops. The remote sensing by satellite and aircraft is employed in order to obtain the information regarding the growth of crops. Although the data from satellites can include wide-range image each time, it is insufficient due to the fixed orbital path of satellites. Therefore, fixed-point observations cannot be sufficiently performed. Moreover, the observations on fixed orbital path cannot be always carried out because of cloud. Although aircrafts are used for the interpolation of the insufficient data by satellites, manned aircrafts need high personnel expenses and maintenance costs. Thereupon, unmanned aerial vehicle (UAV) is recently employed. The objective of the present study is the development of the system to generate the interpolated image data by normalized difference vegetation index (NDVI) map taken by small-type UAV (sUAV), which is low-priced and simple system to implement precision agriculture. The following three assignments have been concretely performed in the present study; 1) light-weight four-band multispectral camera carried in sUAV will be developed, 2) sUAV is operated and the image data will be taken, and 3) NDVI map will be generated from the image data by sUAV and interpolated image data will be also developed to contribute precision agriculture. Consequently, the lightest four-band multispectral camera in the world has been developed, and also sUAV has been able to be successfully operated and acquired image data could also generates NDVI maps.**

## I. Introduction

Precision agriculture is the generic term of the innovative management strategy for agricultural land suggested in 90's. The following cases had been, for example, achieved such as the managements for the dispersion based on the data of crop growth, the advancement of the harvest quantity and quality, and the relief of the load for environment based on the management of the distribution quantity of agrichemicals[1]. The united states of america principally implicates the precision agriculture for a large scale farming to enrich the production, the prevalence of the precision agriculture is the best in the world. On the other hand, Europe area performs the precision agriculture for the environmental preservation as the primary objective. Especially, Germany, United Kingdom, Denmark, and France actively introduce the precision agriculture. Now, although Japan is falling behind USA and Europe regarding the introduction of the precision agriculture, the technical development has been being progressed by Ministry of Agriculture, Forestry, and Fisheries with the initiative in order to incarnate the Japanese-type precision agriculture[2]. Its goal is the veer of the estimation manner of crop growth from the visual inspection to that using the quantitative data. The developing content is roughly classified into four groups, 1) observation tool (the system to grasp crop growth using field server and the remote sensing on satellite), 2) control system (the system to automatically adjust the quantity of compost and manure), 3) harvest tool (the combine harvester to be able to automatically measure the harvest quantity of rice crop and the moisture of rice in the husk), and 4) analysis tool (the information analysis system based on the visualization of harvest quantity to be able to apply to farming

[*]Associate Professor, Graduate School of Engineering. Senior member AIAA.
[†]Graduate Student.
[‡]Bachelor Student.
[§]Professor, Member AIAA.

schedule). The present study will focus on 1) observation tool and 4) analysis tool in order to enrich the Japanese-type precision agriculture from the region of the mechanical engineering.

The Normalized Difference Vegetation Index (NDVI)[3], which represents the activity and distribution of vegetation, is generally employed as the typical quantitative data for the estimation indicator of crop growth. NDVI uses the reflection characteristics of the light on vegetation. NDVI is generated from the observation data which is obtained by the aerial photography using satellites and aircrafts as the remote sensing in a narrow sense. As the remote sensing using satellites repeatedly collects the observation data at a wide area and an identical position, the transition of vegetation on ground can be obtained in detail for a long period. However, the observation using satellites has disadvantages as, 1) a photography cannot be performed for an optional time and position due to always moving the constraint of its orbital path, 2) it has an influence of cloud, and 3) the cost of data is expensive. In fact, even when the cheapest operation will be selected, the minimum order area is 25 [$km^2$] at a new time and the photography cost is roughly 5,000 dollars although it depends on the quantity of cloud. Even the average area of cultivated land of a farming family at the field of Japanese prosperous location is only 1% of its minimum order area. The disadvantage regarding the minimum order area is the major factor to obstruct the employments of satellites. But, as the interpolation of image data using aircrafts resolves the disadvantage, the practical operations using aircrafts has been performed. When a manned aerial vehicle is operated, the personnel and running costs are unfortunately necessary, and the location for takeoff and landing should be secured. In addition, it has restraint with superlative ease regarding the above ground level of 250 [m] due to the Japanese aviation law. Therefore, unmanned aerial vehicle (UAV) is actively employed in the field of remote sensing.

UAV in U.S.A. is already operated for the observations of pasture and crops in the field of agriculture[4,5]. The research and development for the mapping of vineyard are carried out in Australia[6,7]. The research and development for the operation of small-type UAV (sUAV) to flexibly receive the precision agriculture is implemented in U.K.[8], Italia[9], Serbia[10], Switzerland[11], *etc.* at E.U. Spain especially studies to embed the thermal data in multispectral image data[12]. On the other hand, Japan has the following situations regarding sUAVs. The University of Tokyo[13,14] and Hokkaido University[15,16] has been implemented the generation of NDVI map by using sUAVs. In addition, Yanmar Heli & Agri Co., Ltd. begins commercial utilization to generate the database for agricultural land using 200 unmanned helicopters from 2012. When the sizes of bodies and carried cameras are compared, bodies are not downsized, although recent cameras tend to be downsized. Therefore, it anticipates that the acquisition of manipulation techniques and maintenance costs.

The objective of the present study is the generation of NDVI map under the condition of simple operation and the identification of practicability regarding the system for generating NDVI map. Therefore, the following subjects will be focused.

1. a small-size multispectral camera which can carries on sUAV is developed.
2. the image data for the generation of NDVI map is obtained through the operation of sUAV with a multispectral camera.
3. NDVI map is generated and is overlapped on ground image data to offer to precision agriculturists.

The low-cost observation system which is available for the contribution toward the Japanese-type precision agriculture will be constructed.

## II. Outline of System for Generation of NDVI Map

### A. sUAV

The converted sUAV in order to carry multispectral cameras, which is based on the commercial radio-controlled body with fixed wing made by Musashino Model Airplane Laboratory Japan, is used. The outward of the present sUAV "Prairie" is shown in Fig. 1. This body drived by electric motor is selected in order to avoid the pollution of exhaust gas for optical system in the case of internal combustion engines. The specification of Prairie is the span length of 1,180 [mm], the total length of 880 [mm], the weight of 1,027 [g] (maximum weight with several optional parts), and the confirmed weight of carriable payload of roughly 300 [g] (this payload weight is not upper limitation). The original body of Prairie has aileron from wing root to tip. This body is 09-10 class (the displacement volume is from 0.09 to 0.10 [$in^3$]), whose class is minimum size class in engine-installed model airplanes. When a multispectral camera can be carried on the body of 09-10 class, its camera can be carried on other model airplanes of over classes. Prairie has several conversions as the addition of the cargo space in the bottom of the body to carry the multispectral cameras and the

**Figure 1. Exterior of utilized sUAV as Prairie. The bottom right is the enlarged figure around the camera mount.**

addition of the reinforcement around the multispectral cameras. In addition, the aileron is cut in half for spanwise direction and servo motor is installed so that the flap is made from inboard aileron in order to receive the extension of runway distance due to the increase of the weight. The wing becomes to be screwed on the fuselage instead it is fixed by using rubber band in order to increase the strength around the wing root. The propeller and motor become large-size those in order to increase thrust. The position of battery for the multispectral cameras will be shifted for the shift of the center of gravity due to the installation of the multispectral cameras. The polystyrene cover is installed around the camera mount in order to reduce drag shown in Fig. 1. The pocket body warmer is on the battery for the body before flight test so that it can work under the condition of low temperature (under -5 [°C]). The landing gears are converted into skies so as to perform takeoff and landing on snow.

### B. Multispectral Camera

NDVI is the vegetation index which utilizes the optical properties. Figure 2 shows the optical properties that the reflectance is low at visible-red region due to the absorption zone of the chlorophyll and the reflectance is high at near-infrared. That is, NDVI characteristically has high value when the plant cell is vigorous. The

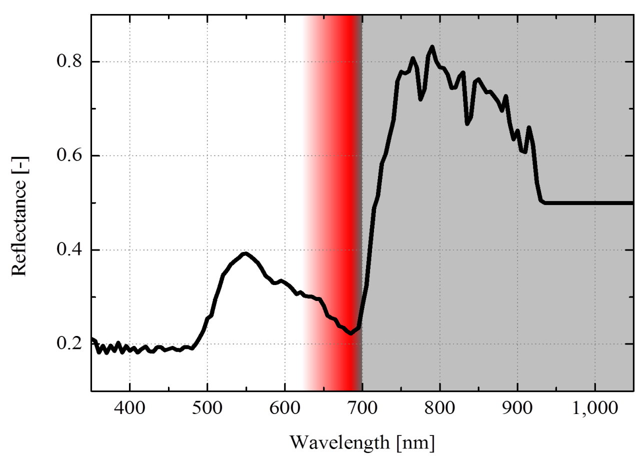


**Figure 2. Reflectance of vegetation. Red region shows VIR (visible red) and grey region shows NIR (near-infrared).**

value of NDVI $V_{\mathrm{NDVI}}$ is the following equation.

$$V_{\mathrm{NDVI}} = \frac{V_{\mathrm{NIR}} - V_{\mathrm{VIR}}}{V_{\mathrm{NIR}} + V_{\mathrm{VIR}}}, \quad (1)$$

where, $V_{\mathrm{NIR}}$ describes the reflectance value of near-infrared and $V_{\mathrm{VIR}}$ denotes the reflectance value of visible red. RGB (red, green, and blue) image data is divided into each color data in the present transformation and the image data for red is generated. The image data for red is superimposed on that for near-infrared so that NDVI is computed on each pixel. The two charge-coupled device (CCD) board cameras as MS-94KR for RGB image data and MS-94LR for monochromatic image data made by Moswell Co., Ltd. are employed because it is suitable size to carry on Prairie. These CCD board cameras are mounted on a circuit shown in Fig. 3. As the objective in the present study is the generation of NDVI map, the necessary data is two as the image data at near-infrared and visible red regions. The optical filters to intercept from the light under the wavelength of 640 [nm] and from the light of infrared are added to MS-94KR in order to simply obtain the image data at visible red region. And also, the long-pass optical filter to intercept from the light over the wavelength of 760 [nm] is added to MS-94LR in order to transmit near-infrared. The light over the wavelength of 900 [nm] is considered as error because of the characteristic to decline the sensitivity of the cameras. The generated circuit with two cameras is installed in case and it carries on the underside of Prairie shown in Fig. 3(a). The block diagram of the developed multispectral cameras shown in Fig. 3(b) indicates that two cameras output data buses, vertical/horizontal synchronizing signals, and pixel clocks to a complex programmable logic device (CPLD). There is no synchronization between two cameras. Therefore, the data buses and pixel clocks from two cameras are simultaneously switched, and the data of RGB/near-infrared image data is put in a static random access memory (SRAM) one after another. There is no correspondence between vertical and horizontal synchronizing signals because image data can be generated from data buses and pixel clocks due to the constant quantity of one image data. A sole CPLD receives the image data from two cameras so that SRAM can be in common. Therefore, the advantages are carried out that the area of the circuit/the power consumption/the total weight can be reduced and the design can be simple, although data cannot be obtained simultaneously. A peripheral interface controller (PIC) extracts the data from SRAM and records it on SD memory card after the preservation to SRAM. A sequence of this work is repeated. The record on SD memory card takes roughly 20 [sec], which is the most quick time to obtain one image data. Although the software can control the time to obtain one image data, the most quick time depends on the condition of write-sectors in SD memory card. As a result, the developed camera system has the weight of 193 [g], which is the lightest system to generate NDVI map in the world shown in Table 1.

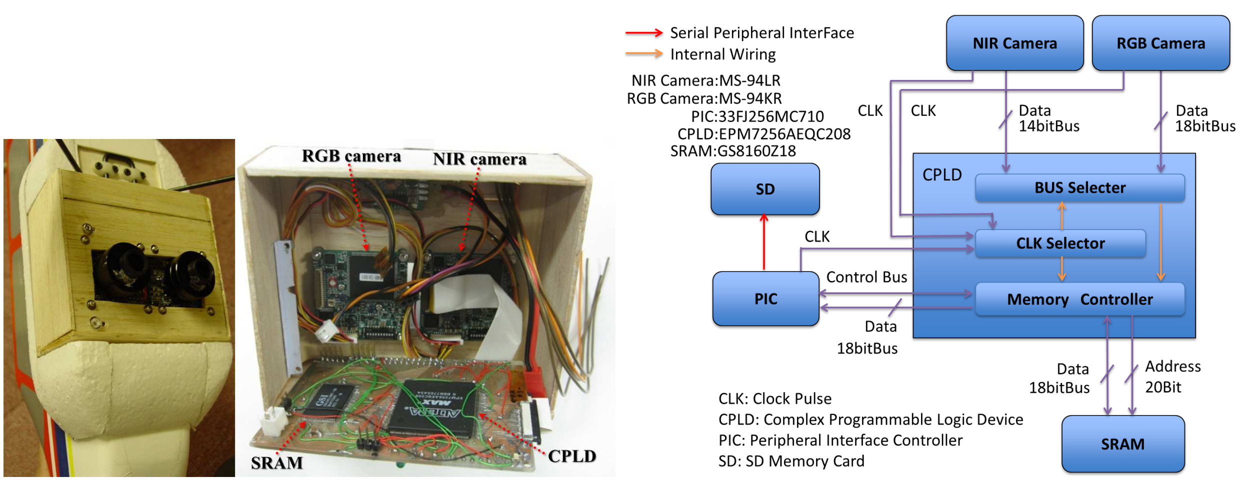


(a) (b)

**Figure 3. Developed multispectrum camera, (a) cameras themselves stored in case and peripheral devices, (b) block figure.**

**Table 1. Published data for carried camera and weight of UAV employed by the institutions of each country.**

| *institution* | *type* | *published year* | *weight [g]* camera | *weight [g]* UAV | *note* |
|---|---|---|---|---|---|
| The University of Tokyo (Japan)[14] | fixed wing | 2005 | 1,000 | 2,000 | digital camera ×2 |
| Hokkaido University (Japan)[15] | helicopter | 2005 | 1,620 | 63,000 | DuncanTech MS2100 |
| University of Applied Sciences and Arts (Switzerland)[11] | helicopter | 2006 | 1,170 | 6,000 | RGB770 [g], CNIR400 [g] |
| The University of Tokyo (Japan)[13] | helicopter | 2008 | 2,000 | 3,300,000 | (RGB, CNIR)×2 |
| Aberystwyth University (UK)[8] | fixed wing | 2008 | 1,470 | 2,700 | |
| University of Applied Sciences and Arts (Switzerland)[11] | quadcopter | 2008 | 350 | 900 | only RGB |
| Institute for Sustainable Agriculture (Spain)[12] | helicopter + fixed wing | 2009 | 2,700 | 6,200 | 6bands |
| University of Novi Sad (Serbia)[10] | paraglider | 2009 | 470 | 5,600 | MCA |
| University of Novi Sad (Serbia)[10] | paraglider | 2009 | 420 | 5,600 | ADC multispecral camera |
| USDA-Agricultural Research Service (USA)[4] | fixed wing | 2010 | 1,240 | 10,000 | FinePix S3PRO UVIR |
| University of Tasmania (Australia)[6] | octocopter | 2011 | 531 | 2,500 | Canon 550D digital SLR |
| The University of Queensland (Australia)[7] | fixed wing | 2012 | 708 | 3,900 | (camera, lens) ×2 |
| Consiglio Nazionale delle Ricerche (Italia)[9] | hexacopter | 2012 | 200 | 2,500 | ADC-lite(no battery) |
| University of Tasmania (Australia)[6] | hexacopter | 2012 | 200 | 2,500 | ADC-lite(no battery) |
| Hokkaido Institute of Technology (Japan) | fixed wing | 2013 | 193 | 1,027 | 4bands, built-in battery |

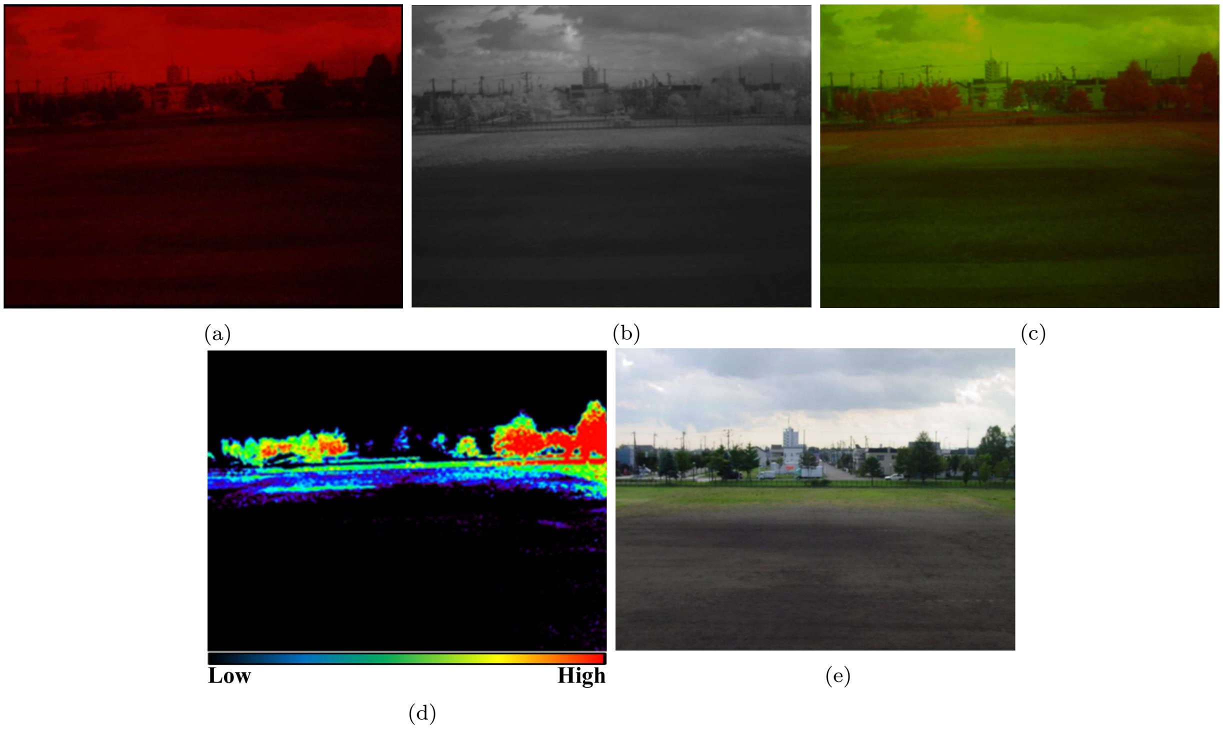


**Figure 4. NDVI map and its attendant images generated in ground test, (a) image for VIR, (b) image for NIR, (c) composite image for intermediate transaction, (d) NDVI map, and (e) RGB image data at identical position.**

## III. Experiment of Multispectral Cameras on the Ground for Advance Preparation

The NDVI map is generated from the image data of multispectral cameras on the ground as the experiment of advance preparation for aerial photography. The intervals of the photography is set to be 30 [sec] due to the easy operation. The brightness of the image data is controlled by the number of the filters. Figure 4 shows the operation verification of the multispectral cameras and the image processing. The multispectral cameras takes the image data of visible red region shown in Fig. 4(a) and that of near-infrared region shown in Fig. 4(b). The composite image data shown in Fig. 4(c) is prepared in order to deal with the monochromatic image data. The prepared composite image data is made from Fig. 4(a) which visible red is transposed with visible green and Fig. 4(b) which near-infrared is transposed with visible red. The generated NDVI map is shown in Fig. 4(d). The high value (red) shown in Fig. 4(d) describes that photosynthesis is active, in contrast, the low value (black) describes that photosynthesis is inactive. The RGB image data at the identical position is shown in Fig. 4(e) in order to confirm that the generated NDVI map accords with the physical environment. Figure 4(e) takes the sky, trees and structures, green, and ground from the upside. NDVI map shown in Fig. 4(d) at the sky, structures, and ground which cannot photosynthesize has black, in contract, it at trees and green is not black. Especially, the color for dying green indicates the low value of NDVI. Consequently, the generated NDVI map shown in Fig. 4(d) accords with the physical environment and all of the process for the generation of NDVI map is successfully carried out.

## IV. Experiment of Aerial Photography

### A. Generation of NDVI map

The aerial photography is performed by using Prairie with the multispectral cameras, and then the image data at roughly 20 positions is successfully obtained. The image data at a typified position is shown as the result in the present study. Figure 5 shows the image data of visible red (Fig. 5(a)) and near-infrared (Fig. 5(b)) regions, the generated NDVI map (Fig. 5(c)), RGB map by GoogleEarth (Fig. 5(d)) to compare with the

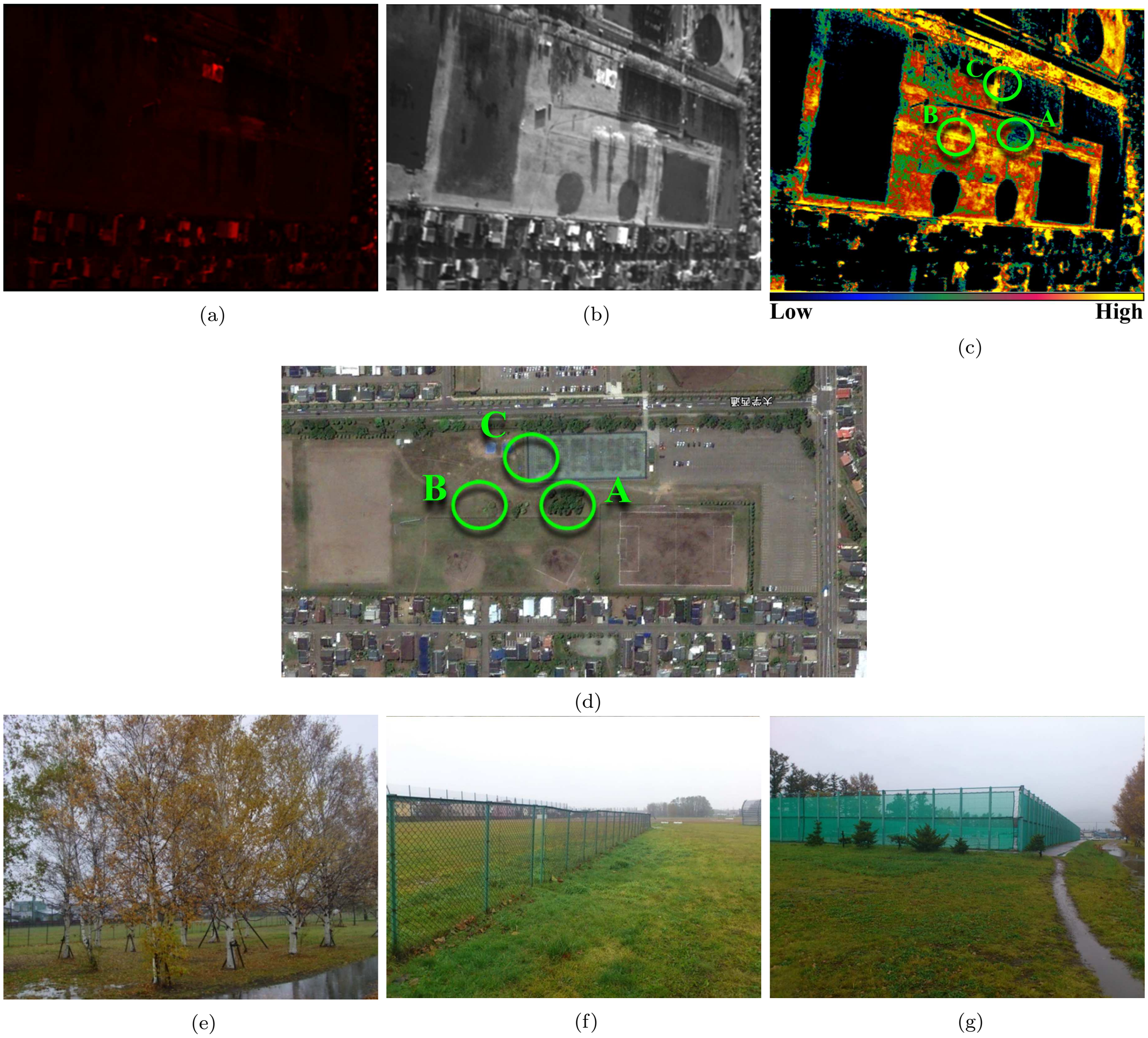


**Figure 5. NDVI map and its attendant images generated in aerial-shooting test, (a) VIR image, (b) NIR image, (c) generated NDVI map, (d) RGB image data in the vicinity of shooting position from GoogleEarth, (e) RGB image on the ground at position A in Figs. (c) and d, (f) RGB image on the ground at position B in Figs. (c) and d, and (g) RGB image on the ground at position C in Figs. (c) and (d).**

NDVI map (Fig. 5(c)), and RGB image data on the ground at three characteristic locations (Fig. 5(e), (f), and (g)) in the NDVI map (Fig. 5(c)) and RGB image data by GoogleEarth (Fig. 5(d)). As this figure can takes a large examination area, it is appropriate for the verification of configuration as the problem that aerial photography generally has. Figures. 5(a) and (b) show that the image data of visible red and near-infrared can be sharply obtained. Therefore, NDVI map shown in Fig. 5(c) can be successfully generated. Figures 5(c) and (d) are verified as the identical location because the arrangements of the tennis court and the grounds for succor and softball correspond between Figs. 5(c) and (d), and also because there is no place with those arrangements in the vicinity of the present experimental area. Figures 5(c) and (d) are compared so that the precision of Fig. 5(c) is verified. The locations of A, B, and C with essential characteristics shown in Figs. 5(e), (f), and (g) are especially selected identified in Figs. 5(c) and (d). Those characteristics are as follows; A) although NDVI is low value in Fig. 5(c), vegetation can be confirmed in Fig. 5(d), B) although the high value of NDVI is distributed in a belt in Fig. 5(c), the vegetation distribution is uniform in Fig. 5(d), and C) there is an artificial object with green color. Figure 5(e) as the RGB ground image data at the location A indicates that there are ginkgo trees with autumn colors in the leaves. Thus, there is the time difference regarding the photographing season between Figs. 5(c) and (d). Since Fig. 5(c) as NDVI map

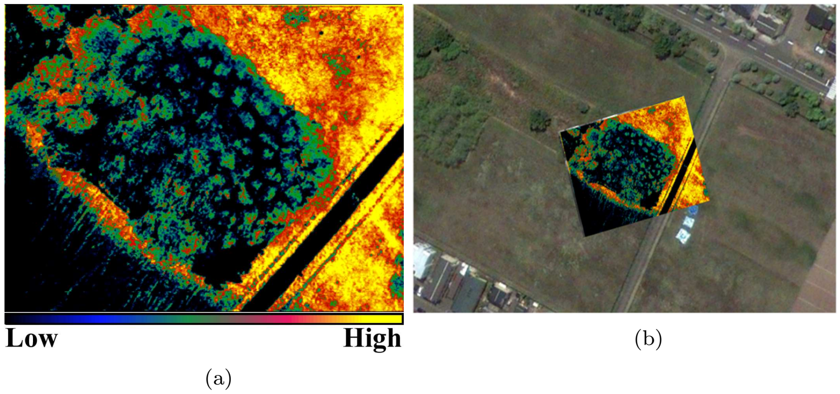


**Figure 6. RGB image data on which NDVI map is overlapped at characteristic topography, (a) NDVI map, (b) overlapped RGB image.**

is generated by using the multispectral image data taken in the autumn, NDVI becomes low value. On the other hand, as Fig. 5(d) as RGB aerial image data by GoogleMap may be taken in the summer, the trees with verdant leaves takes. Therefore, NDVI map at location A describes precision information regarding vegetation environment. Figure 5(f) as the RGB ground image data at the location B indicates that there is the vegetation with vigor around a fence. Therefore, the high value of NDVI is distributed in a belt in Fig. 5(c) at location B. As a result, NDVI map can describes the particular distribution of photosynthetic activity which the RGB aerial image data cannot describes. Figure 5(g) as the RGB ground image data at the location C indicates that there is a large fence which can be seen in Fig. 5(d) as RGB aerial image data. Although Fig. 5(d) as the RGB aerial image data shows green color at the location C, as Fig. 5(c) has black color, NDVI map surely indicates no photosynthetic activity. Therefore, the analysis error regarding NDVI due to the artificial object with green color does not occur. Consequently, the generated NDVI map corresponds to the real environment and NDVI is analyzed and visualized with high precision.

### B. Overlap of NDVI map on RGB Aerial Image Data

The image data to overlap NDVI map on RGB aerial image data by GoogleMap is generated because overlap image data is a general presentation medium to the persons to engage in precision agriculture. Figure 6 shows one of the overlap image data and overlapped NDVI map. As the overlap is manually operated by using three characteristic points in image data, the narrow-range image data which takes characteristic configurations is selected. Note that NDVI map shown in Fig. 6(a) is manually molded regarding the slant and the scale in order to overlap on the RGB aerial image data. Figure 6(b) indicates that the NDVI map and the RGB aerial image data are the identical location because path, fence, and the boundary of trees correspond between them, although there is difference of the photosynthetic activity of threes due to photographic season. Consequently, generated NDVI map is useful for persons to engage in precision agriculture because overlap image data can be successfully generated.

Note that the several problems should be resolved in order to efficiently generate overlap image data. A global positioning system (GPS) will be carried on body in order to obtain flight data and the software for image processing will be also developed so that the slant of NDVI map is automatically molded and characteristic points are automatically extracted.

## V. Conclusions

The low-cost observation system in order to contribute toward the Japanese-type precision agriculture was constructed in the present study. As a result, the lightest small-size multispectral camera in the world which carries on a small-type unmanned aerial vehicle has been developed. The image data for visible red and near-infrared to generate normalized difference vegetation index map has been obtained through the operation of a small-type unmanned aerial vehicle with a small-size multispectral camera. Moreover, normalized difference vegetation index map which corresponds to real environment has been successfully generated and has been overlapped on ground image data. The generated normalized difference vegetation index is analyzed and visualized with high precision. The developed lightest multispectral camera can be advantageously utilized regarding the flexibility for the selection of unmanned aerial vehicle and for the operation of body. Operational environment to automatically generate normalized difference vegetation index will be developed so that more effective Japanese-type precision agriculture is realized.

## Acknowledgment

The present study was supported in part by Mr. Shun Nakahara and Sapporo Akashia Model Club.

## References

[1]Umeda, M., "Precision Agriculture in Foreign Countries," *Journal of Japan Association for Techno-Innovation in Agriculture, Forestry and Fisheries(in Japanese)*, Vol. 30, No. 5, 2007, pp. 40–44.

[2]Agriculture, F., Fisheries Research Council, Ministry of Agriculture, F., and in Japan, F., "Technological Development for Japanese-Type Precision Agriculture," *Research and Development Report for Agriculture, Forestry and Fisheries No.24(in Japanese)*, 2008, pp. 1–17.

[3]Lelong, C., Burger, P., Jubelin, G., Roux, B., Labbes, S., and Baret, F., "Assessment of Unmanned Aerial Vehicles Imagery for Quantitative Monitoring of Wheat Crop in Small Plots," *Sensors*, Vol. 8, No. 5, 2008, pp. 3557–3585.

[4]Hunt, E., Hively, W., Fujikawa, S., Linden, D., Daughtry, C., and McCarty, G., "Acquisition of NIR-Green-Blue Digital Photographs from Unmanned Aircraft for Crop Monitoring," *Remote Sensing*, Vol. 2010, No. 2, 2010, pp. 290–305.

[5]Laliberte, A., Herrick, J., Rango, A., and Winters, C., "Acquisition, Orthorectification, and Object-Based Classification of Unmanned Aerial Vehicle (UAV) Imagery for Rangeland Monitoring," *Photogrammetric Engineering and Remote Sensing*, Vol. 76, No. 6, 2010, pp. 661–672.

[6]Turner, D., Lucieer, A., and Watson, C., "Development of an Unmanned Aerial Vehicle (UAV) for Hyper Resolution Vineyard Mapping Based on Visible, Multispectral, and Thermal Imagery," *Proceedings of 34th International Symposium on Remote Sensing of Environment*, 2011.

[7]Lechner, A., Fletchera, A., Johansen, K., and Erskinea, P., "Characterising Upland Swamps Using Object-Based Classification Methods and Hyper-Spatial Resolution Imagery Derived from an Unmanned Aerial Vehicle," *International Annals of the Photogrammetry, Remote Sensing and Spatial Information Sciences*, Vol. 1, No. 3, 2012, pp. 101–106.

[8]Gay, A., Stewart, T., Angel, R., Easey, M., Eves, A., Thomas, N., and Kemp, A., "Developing Unmanned Aerial Vehicles for Local and Flexible Environmental and Agricultural Monitoring," *Proceedings of the Remote Sensing and Photogrammetry Society 2009 Annual Conference*, 2009, pp. 471–476.

[9]Primicerio, J., di Gennaro, S., Fiorillo, E., Genesio, L., Lugato, E., Matese, A., and Vaccari, F., "A Flexible Unmanned Aerial Vehicle for Precision Agriculture," *Precision Agriculture*, Vol. 13, No. 4, 2012, pp. 517–523.

[10]Antic, B., Culibrk, D., Crnojevic, V., and Minic, V., "An Efficient UAV Based Remote Sensing Solution for Precision Farming," *BioSense - The First International Workshop on ICT and Sensing Technologies in Agriculture, Forestry and Environment*, 2009.

[11]Nebiker, S., Annen, A., Scherrer, M., and Oesch, D., "A Light-Weight Multispectral Sensor for Micro UAV-Opportunities for Very High Resolution Airborne Remote Sensing," *The International Archives of the Photogrammetry, Remote Sensing and Spatial Information Sciences, Vol.XXXVII-B1*, 2008, pp. 1193–1200.

[12]Berni, J., Zarco-Tejada, P., Suarez, L., and Fereres, E., "Thermal and Narrowband Multispectral Remote Sensing for Vegetation Monitoring from an Unmanned Aerial Vehicle," *IEEE Transactions on Geoscience and Remote Sensing*, Vol. 47, No. 3, 2009, pp. 722–738.

[13]Nagai, M., Chen, T., Ahmed, A., and Shibasaki, R., "UAV Borne Mapping by Multi Sensor Integration," *The International Archives of the Photogrammetry, Remote Sensing and Spatial Information Sciences, Vol.XXXVII-B1*, 2008, pp. 1215–1221.

[14]Suzuki, S., "Application of Unmanned Aerial Vehicle to the Research and Education in University," *Aeronautics and Space 670(in Japanese)*, 2009, pp. 6–12.

[15]Ishii, K., Sugiura, R., Fukagawa, T., Noguchi, N., and Shibata, Y., "Crop Status Sensing System by Multi-Spectral Imaging Sensor (Part 1)," *Journal of the Japanese Society of Agricultural Machinery(in Japanese)*, Vol. 68, No. 2, 2006, pp. 33–41.

[16]Hanya, I., Ishii, K., and Noguchi, N., "Estimation of Moisture Content of Wheat Ear Using Satellite and Helicopter Imagery," *Environmental Information Science 23(in Japanese)*, 2011, pp. 155–160.